Downregulation of miR-10b-5p facilitates the proliferation of uterine leiomyosarcoma cells: A microRNA sequencing-based approach

KOSUKE YOSHIDA[1-3], AKIRA YOKOI[1,2], MASAMI KITAGAWA[4], MAI SUGIYAMA[4], TOMOFUMI YAMAMOTO[3], JUN NAKAYAMA[3], HIROSHI YOSHIDA[5], TOMOYASU KATO[6], HIROAKI KAJIYAMA[1] and YUSUKE YAMAMOTO[3]

[1]Department of Obstetrics and Gynecology, Nagoya University Graduate School of Medicine; [2]Institute for Advanced Research, Nagoya University, Nagoya, Aichi 466-8550; [3]Laboratory of Integrative Oncology, National Cancer Center Research Institute, Tokyo 104-0045; [4]Bell Research Center, Department of Obstetrics and Gynecology Collaborative Research, Nagoya University Graduate School of Medicine, Nagoya, Aichi 466-8550; Departments of [5]Diagnostic Pathology and [6]Gynecology, National Cancer Center Hospital, Tokyo 104-0045, Japan

Received October 7, 2022; Accepted February 2, 2023

DOI: 10.3892/or.2023.8523

Abstract. Uterine leiomyosarcoma (ULMS) is one of the most aggressive gynecological malignancies. In addition, the molecular background of ULMS has not been fully elucidated due to its low incidence. Therefore, no effective treatment strategies have been established based on its molecular background. The present study aimed to investigate the roles of microRNAs (miRNAs/miRs) in the development of ULMS. Comprehensive miRNA sequencing was performed using six ULMS and three myoma samples, and revealed 53 and 11 significantly upregulated and downregulated miRNAs, respectively. One of the most abundant miRNAs in myoma samples was miR-10b-5p. The mean normalized read count of miR-10b-5p was 93,650 reads in myoma, but only 27,903 reads in ULMS. Subsequently, to investigate the roles of miR-10b-5p, gain-of-function analysis was performed using SK-UT-1 and SK-LMS-1 cell lines. The overexpression of miR-10b-5p suppressed cell proliferation and reduced the number of colonies. Moreover, miR-10b-5p increased the number of cells in the G_1 phase. In conclusion, tumor-suppressive miR-10b-5p was significantly downregulated in ULMS compared with in myoma; thus, miR-10b-5p may serve a specific role in sarcoma progression.

Correspondence to: Dr Akira Yokoi, Department of Obstetrics and Gynecology, Nagoya University Graduate School of Medicine, 65 Tsuruma-cho, Showa-ku, Nagoya, Aichi 466-8550, Japan
E-mail: ayokoi@med.nagoya-u.ac.jp

Dr Yusuke Yamamoto, Laboratory of Integrative Oncology, National Cancer Center Research Institute, 5-1-1 Tsukiji, Chuo-ku, Tokyo 104-0045, Japan
E-mail: yuyamamo@ncc.go.jp

Key words: uterine leiomyosarcoma, microRNA sequencing, miR-10b-5p, proliferation, cell cycle

Introduction

Uterine leiomyosarcoma (ULMS) is a lethal gynecological malignancy. The annual incidence of ULMS is ~0.86 per 100,000 women worldwide (1-3). Surgical resection is the best treatment option for localized ULMS; however, the majority of cases eventually result in recurrence (2-4). There are currently no effective treatment strategies for recurrent and metastatic ULMS (2). Notably, the Food and Drug Administration has approved new therapeutic agents, such as trabectedin and pazopanib, for soft-tissue tumors in the past decade (3). However, the prognosis of patients with advanced/recurrent ULMS remains unsatisfactory (5-7). Several clinical trials have reported that the median progression-free survival time of advanced/recurrent ULMS is approximately a few months, and the median overall survival time is within 2 years (5-7). Therefore, the development of new therapeutic agents is required in the clinical setting.

Until recently, the molecular biological characteristics of soft-tissue tumors, including ULMS, were poorly understood due to their low incidence. However, the development of next-generation sequencing may improve understanding of the characteristics of ULMS and other malignancies. Several genomic analyses have identified frequently mutated genes in ULMS, including alterations that affect *TP53*, *RB1*, *ATRX* and *PTEN* (8-11). Moreover, transcriptome analyses have revealed that cell cycle-related kinase activation is a dominant feature of ULMS (12,13). Notably, the roles of microRNAs (miRNAs/miRs) in ULMS development remain unclear. miRNAs are small non-coding RNAs ~22 nucleotides in length, and >2,000 annotated mature miRNAs are present in the human genome (14-16). Functionally, miRNAs post-transcriptionally regulate the expression of their target gene, and a miRNA potentially has multiple target genes, depending on

cell type (17-19). Thus, miRNAs serve critical roles in cancer development by modulating fundamental biological processes. ULMS research has reported the inverse correlation between let-7c and *HMGA2* in clinical samples and has experimentally validated the tumor-suppressive effect of let-7c (20). Moreover, miR-152 has been reported to suppress ULMS cell proliferation by regulating *MET* expression (21). Therefore, anomalous miRNA expression may contribute to ULMS development; however, the significance of the majority of miRNAs remains to be determined.

The present study performed comprehensive miRNA sequencing to investigate unique miRNA profiles of ULMS. Subsequently, the study focused on miR-10b-5p and evaluated its potential functions in LMS-derived cell lines.

Materials and methods

Patients. Medical records from the National Cancer Center Hospital (Tokyo, Japan) were retrospectively reviewed. Excluding patients without written informed consent, all six patients with ULMS who underwent surgery without neoadjuvant therapy between January 2011 and September 2020 were included. The archival fresh-frozen tumor and adjacent normal tissues of these patients, which were stored at the National Cancer Center Biobank (Tokyo, Japan), were used in the present study. Moreover, three leiomyoma tissues from three other patients were used as controls. The case number corresponds to the case number from our previous report (13). The clinical information, such as age, stage, mitotic rate and the presence of necrosis, was obtained from their clinical records. The International Federation of Gynecology and Obstetrics staging system was used (2,3). The study protocol was approved by the ethics committee of the National Cancer Center (approval no. 2020-160). Written informed consent was obtained from all patients. Moreover, the study was carried out according to The Declaration of Helsinki.

Comprehensive miRNA sequencing. Total RNA was extracted using the miRNeasy Mini Kit (Qiagen GmbH), and small RNA libraries were prepared using the NEBNext Multiplex Small RNA Library Prep Set for Illumina (cat. no. E7300L; New England Biolabs, Inc.) according to the manufacturers' protocol. Subsequently, the small RNA libraries were separated by electrophoresis (120 V, 60 min) on a 10% TBE gel (cat. no. EC6265BOX; Thermo Fisher Scientific, Inc.), and DNA fragments corresponding to 140-160 bp (the lengths of small non-coding RNA plus the 3' and 5' adaptors) were recovered. The cDNA concentration was then measured using the Qubit dsDNA HS Assay Kit and a Qubit2.0 Fluorometer (Thermo Fisher Scientific, Inc.). Finally, single-end reads were performed using the MiSeq Reagent Kit v3 (cat. no. MS-102-3001; Illumina, Inc.) on the Illumina MiSeq (Illumina, Inc.) and the loading concentration of the final library was 10 pM.

The CLC Genomics Workbench version 9.5.3 program (Qiagen GmbH) was used for adaptor trimming and mapping to the miRbase 21 database (https://www.mirbase.org/) without allowing any mismatch. After normalization using reads per million mapped reads, low-expressed miRNAs (<10 reads in all samples) were excluded from further analyses. Subsequently, RStudio (RStudio, Inc.) and R software (version 4.0.3; https://www.r-project.org/) were used. For the heatmap analysis, miRNAs with an absolute log2 (fold change) of >0.8 were extracted and utilized. The data were then converted to base 10 logarithms and z-scores, and the heatmap.2 function of the gplots package (ver. 3.1.0; https://cran.r-project.org/package=gplots) was used. The P-values for each gene were calculated using the Wald test in DESeq2 (ver. 1.30.0) for the volcano plots (22).

Cell culture and miRNA mimics. SK-UT-1 (ULMS-derived cell line) and SK-LMS-1 (vulvar LMS-derived cell line) were purchased from the American Type Culture Collection. The cells were maintained in MEM (Nacalai Tesque, Inc.) containing 10% fetal bovine serum (FBS; Thermo Fisher Scientific, Inc.), 1 mM sodium pyruvate (Thermo Fisher Scientific, Inc.) and penicillin-streptomycin (Thermo Fisher Scientific, Inc.) in a humidified incubator at 37˚C with 5% CO_2. The cell lines tested negative for mycoplasma contamination and were used between 5 and 40 passages for the experiments.

mirVana miRNA mimics (Thermo Fisher Scientific, Inc.) were used to induce overexpression of miRNAs in the present study, and the assay IDs were as follows: miR-10b-5p (MC11108), miR-29a-3p (MC12499), miR-126-3p (MC12841), miR-186-5p (MC11753) and Negative Control (NC) #1 (4464058). Cells were transfected with 20 nM miRNA mimics using Lipofectamine® RNAi Max (Thermo Fisher Scientific, Inc.) at 37˚C for ≥24 h.

Reverse transcription-quantitative PCR (RT-qPCR). Total RNA was extracted from clinical samples or cell lines as aforementioned, and cDNA was synthesized using a TaqMan Advanced miRNA cDNA Synthesis Kit (Thermo Fisher Scientific, Inc.) according to the manufacturers' protocol. Subsequently, qPCR was performed using TaqMan Fast Advanced Master Mix and TaqMan Advanced miRNA Assay (Thermo Fisher Scientific, Inc.); the assay IDs were as follows: miR-10b-5p (478494_miR), miR-29a-3p (478587_miR), miR-126-3p (477887_miR), miR-186-5p (477940_miR) and *RNU6B* (001093). The amplification program was as follows: Denaturation at 95˚C for 10 min, followed by 40 amplification cycles at 95˚C for 15 sec and 60˚C for 60 sec. The amplified product was monitored by measuring the fluorescence intensity of FAM. *U6* was used as a reference gene to normalize the expression and the $2^{-\Delta\Delta Cq}$ method was used for quantification (23).

Cell proliferation assay. Cells were seeded into 96-well plates (1,000 cells/well) and transfected with the miR-10b-5p, miR-29a-3p, miR-126-3p, miR-186-5p or NC mimics. A total of 24, 48 and 72 h post-transfection, cell proliferation was assessed using the CellTiter-Glo 2.0 Cell Viability Assay (Promega Corporation), and luminescence was measured 10 min after adding the reagent using SpectraMax iD3 (Molecular Devices, LLC) or Infinite 200 PRO (Tecan Group, Ltd.). Experiments were performed in triplicate and repeated three times.

Clonogenic assay. Cells were transfected with miR-10b-5p or NC mimic in 35-mm dishes (50,000 cells/dish). A total of 24 h post-transfection, the cells were seeded into six-well plates

(300 cells/well, six replicates) and incubated for 6 days in a humidified incubator at 37˚C with 5% CO_2. Subsequently, the cells were fixed with 4% paraformaldehyde for 10 min and stained with 1% crystal violet for 10 min at room temperature, and the colonies (>50 cells) were manually counted.

Soft agar colony formation assay. For soft agar colony formation assay, 2X MEM was prepared using 10X MEM (cat. no. M0275; MilliporeSigma), FBS, sodium hydrogen carbonate (FUJIFILM Wako Pure Chemical Corporation), GlutaMax (Thermo Fisher Scientific. Inc.), sodium pyruvate and penicillin-streptomycin (Thermo Fisher Scientific, Inc.). Cells were transfected with miR-10b-5p or NC mimic in 35-mm dishes (50,000 cells/dish). Subsequently, 1.6 and 0.6% agar solutions were prepared using agar powder (FUJIFILM Wako Pure Chemical Corporation) diluted with PBS. Prewarmed 2X MEM and melted 1.6% agar solution were mixed (1:1 ratio) and transferred into six-well plates to form the bottom agar layer. Then, a total of 24 h post-transfection, the cells were trypsinized and resuspended in a prewarmed 2X MEM. The cell suspension and melted 0.6% agar solution were mixed (1:1 ratio) and placed on the bottom agar layer (3,000 cells/well). The cells were incubated with culture medium for 14 days in a humidified incubator at 37˚C with 5% CO_2. Then, cells were stained with 0.01% crystal violet for 1 h at room temperature, and the colonies (>50 cells) were manually counted. Images were captured using a WRAYCAM-NF300 light microscope (WRAYMER Inc.).

Cell cycle assay. Cells were transfected with miR-10b-5p or NC mimic in six-well plates (50,000 cells/well). A total of 48 h post-transfection, the cells were harvested trypsinization and washed with 3% FBS in PBS. Then, the cells were fixed in cold 70% ethanol with gentle vortexing and were placed in 70% ethanol at -20˚C for 24 h. The cells were centrifuged at 500 x g for 15 min at 20˚C and resuspended in 3% FBS in PBS. After centrifuging, the cell pellet was stained with 0.5 ml PI/RNase Staining Buffer (BD Biosciences) for 15 min at room temperature. The FACSCanto II flow cytometer (BD Biosciences) was used for cell cycle analysis. The resulting data were analyzed using FlowJo software (version 10.8.1; FlowJo LLC). Experiments were performed in triplicate.

RNA sequencing. Cells were transfected with miR-10b-5p or NC mimic in six-well plates (50,000 cells/dish). A total of 48 h post-transfection, total RNA was extracted as aforementioned. Pair-end sequencing was performed by Azenta Life Sciences. Briefly, total RNA was quantified and qualified using the Qubit RNA HS Assay Kit (Thermo Fisher Scientific, Inc.) and TapeStation RNA ScreenTape (Agilent Technologies, Inc.). To enrich poly-A mRNA and to remove rRNA molecules, the NEBNext Poly(A) mRNA Magnetic Isolation Module (cat. no. E7490L; New England Biolabs, Inc.) was used. Subsequently, cDNA synthesis followed by transcriptome library preparation was conducted using the MGIEasy RNA Directional Library Prep Kit V2.0 (cat. no. 1000005272; MGI Tech Co., Ltd.). The resulting sequencing libraries were quantified using the Qubit DNA HS Assay Kit (Thermo Fisher Scientific, Inc.) and their fragment size distribution was confirmed by TapeStation D1000 ScreenTape (Agilent Technologies, Inc.). The double-stranded library fragments were pooled/multiplexed at an equimolar amount and further processed into single-stranded circular DNA (sscDNA). The sscDNA libraries were quantified using the Qubit ssDNA Assay Kit (Thermo Fisher Scientific), and a 40 fmol sscDNA library pool was used for generating DNA nanoballs (DNBs) by rolling circle replication reaction. DNBs were then loaded into a flow cell for sequencing on the DNBSEQ-G400 platform (MGI Tech Co., Ltd.) with 150 bp paired-end configuration, according to the manufacturer's instructions. From the sequencing data, expression levels for each gene were quantified by Kallisto (ver. 0.46.2) (24). Then, data were summarized using the tximport package (ver. 1.18.0) of R software, and scaled transcript per million counts were used for further analyses (25). Genes with low read coverage (maximum read count, <10 reads) were excluded. Compared with NC-transfected cells, genes with absolute log2 (fold change) >0.8 were considered differentially expressed genes (DEGs). Subsequently, common DEGs in both cell lines were used to generate the heatmap after converting the data to base 10 logarithms and z-scores. The heatmap.2 function of the gplots package (ver. 3.1.0; https://cran.r-project.org/package=gplots) was used. Pathway analysis was performed using the Ingenuity Pathway Analysis (IPA) software (ver. 84978992; Qiagen GmbH).

Statistical analysis. Data are presented as the mean ± standard error of the mean and experiments were performed at least in triplicate and repeated three times. All statistical analyses were performed using RStudio and R software (ver. 4.0.3). Welch's t-test was used to determine the significant differences between the means of two sets of data, and the paired t-test was used to compare the expression of miR-10b-5p in paired ULMS and adjacent normal tissues. $P<0.05$ was considered to indicate a statistically significant difference.

Results

Comprehensive miRNA sequencing. Small RNA sequencing was performed using archival fresh-frozen samples from six patients with ULMS and three patients with myoma. Table I shows the clinical information of the patients. The heatmap shown in Fig. 1A indicated that the miRNA profiles of patients with ULMS were usually different from those of patients with myoma. However, the miRNA profiles were diverse in patients with ULMS; notably, the miRNA expression pattern in ULMS-3 was more similar to that of myoma compared with the other types of ULMS. Our previous study reported that ULMS-3 was characterized by higher *ESR1* expression and a lower mitotic rate than other types of ULMS, suggesting that ULMS-3 is a gynecological subtype and a clinically less aggressive subtype of LMS (13,26,27). Subsequently, a volcano plot that compares ULMS to myoma was generated to investigate ULMS-associated miRNAs. The volcano plot revealed that 53 and 11 miRNAs were significantly upregulated or downregulated, respectively, in ULMS compared with in myoma (Fig. 1B). The normalized read counts of the 64 miRNAs are shown in Table SI. miRNAs with abundant expression were selected according to the baseline expression level. Dot plots of the top four downregulated miRNAs (miR-10b-5p, miR-29a-3p, miR-126-3p and miR-186-5p) and

Table I. Clinical information of patients.

Case	Age, years	FIGO stage	Mitotic rate, cells/10HPF	Necrosis
ULMS-1	58	IB	38	+
ULMS-2	79	IB	15	+
ULMS-3	74	IB	5	+
ULMS-4	61	IIB	40	+
ULMS-5	53	IB	70	+
ULMS-6	55	IB	15	+
Myoma-1	54	-	-	-
Myoma-2	49	-	-	-
Myoma-3	57	-	-	-

FIGO, The International Federation of Gynecology and Obstetrics; HPF, high-power field; ULMS, uterine leiomyosarcoma.

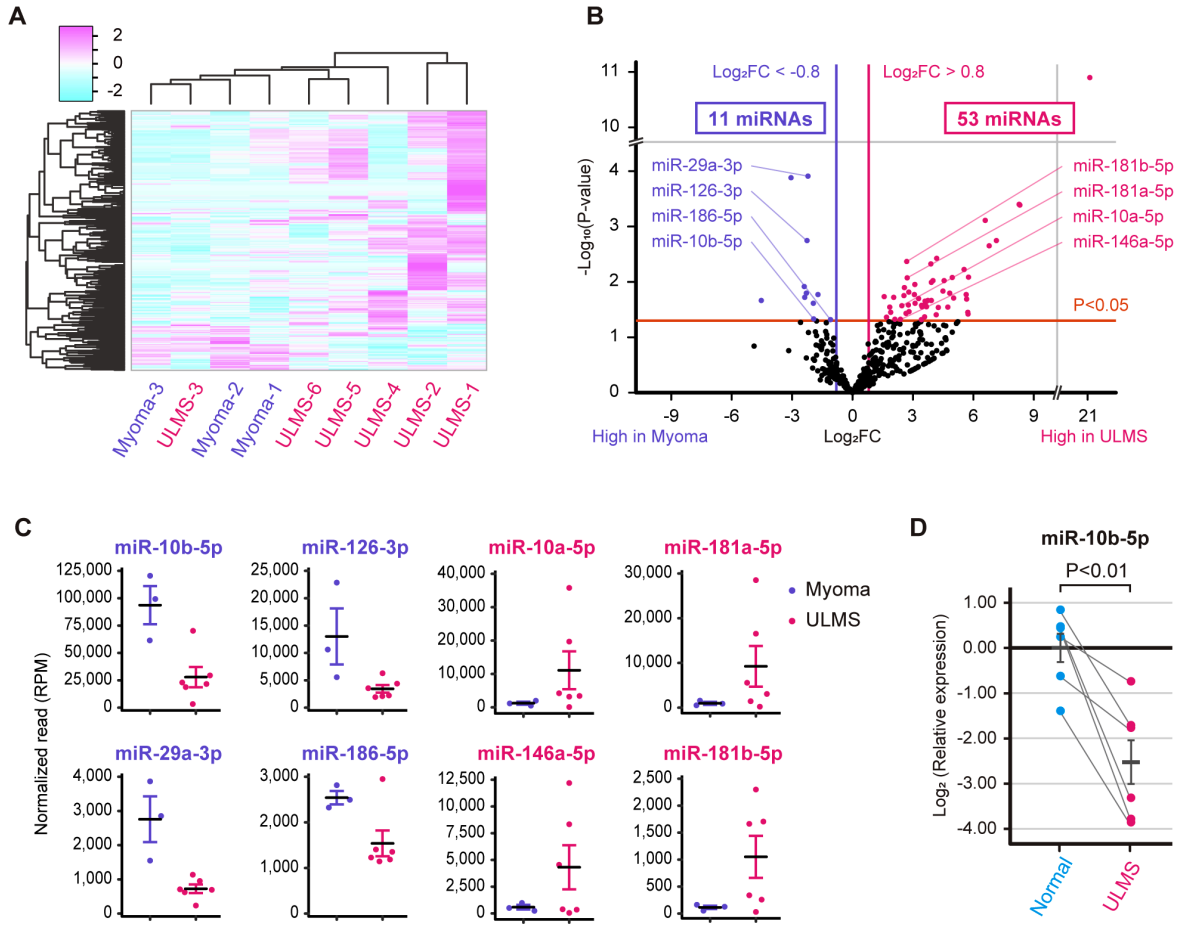

Figure 1. miRNA profiles of ULMS and myoma. (A) Hierarchical clustering and heatmap analysis showing 334 differentially expressed miRNAs between the ULMS and myoma samples. The differentially expressed miRNAs were defined as an absolute log2 FC >0.8. (B) Volcano plot between ULMS and myoma samples. The P-values for each miRNA were calculated using the Wald test in DESeq2. (C) Normalized reads of miR-10b-5p, miR-29a-3p, miR-126-3p, miR-186-5p, miR-10a-5p, miR-146a-5p, miR-181a-5p and miR-181b-5p. (D) Relative expression levels of miR-10b-5p in paired ULMS and myometrium samples. The relative expression was compared using paired Student's t-test. Error bars represent standard errors of the mean. FC, fold change; miR/miRNA, microRNA; RPM, reads per million; ULMS, uterine leiomyosarcoma.

the top four upregulated miRNAs (miR-10a-5p, miR-146a-5p, miR-181a-5p and miR-181b-5p) are shown in Fig. 1C. In particular, the mean normalized read count of miR-10b-5p was 93,650 reads in myoma; however, it was markedly decreased to 27,903 reads in ULMS. Thus, miR-10b-5p was considered to serve a role in ULMS progression. RT-qPCR was performed to validate miR-10b-5p downregulation in ULMS; it was revealed that miR-10b-5p expression was significantly downregulated

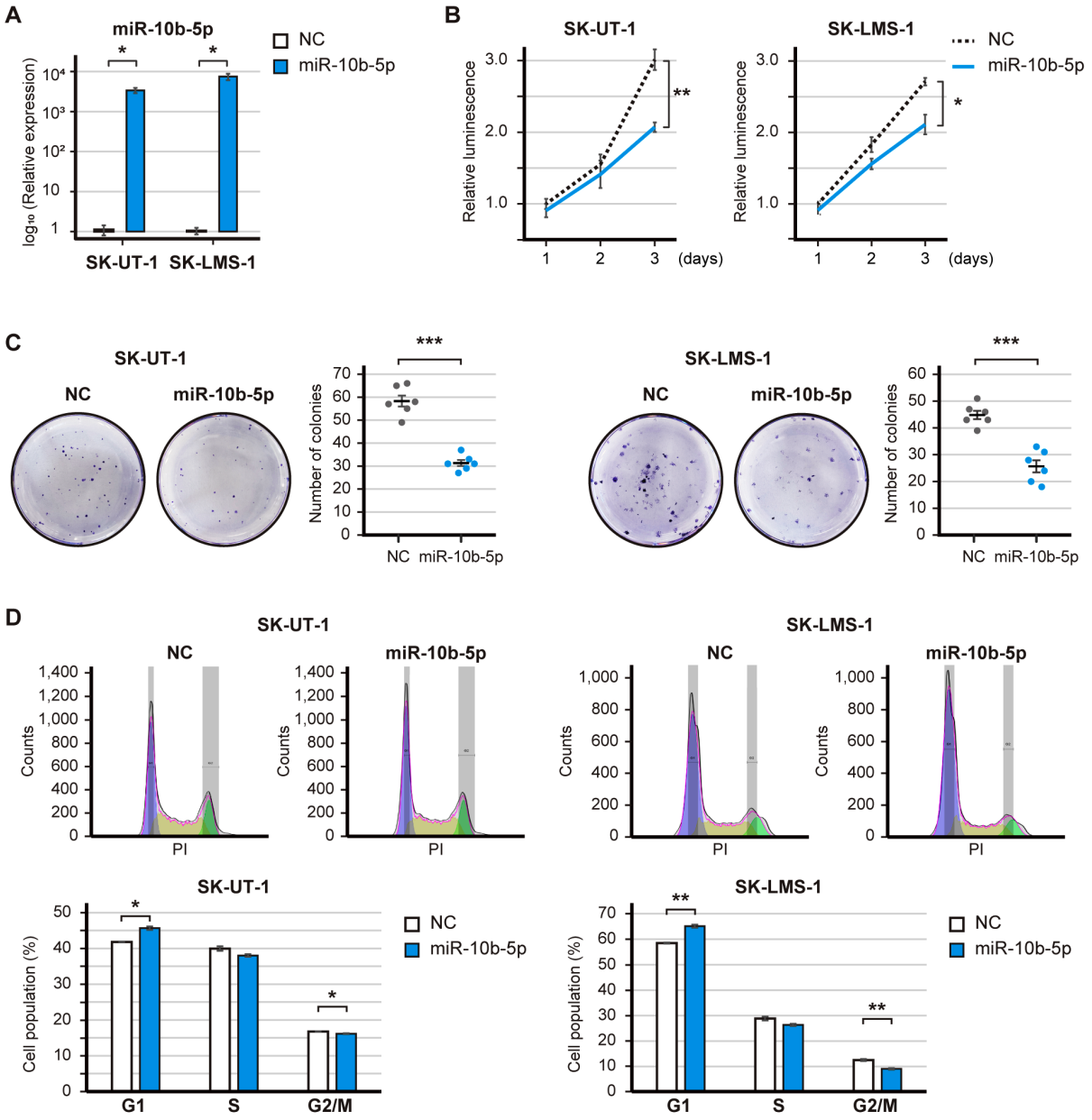

Figure 2. Effect of miR-10b-5p overexpression on leiomyosarcoma-derived cell lines. (A) Validation of miR-10b-5p overexpression following transfection with 20 nM miR-10b-5p mimics. (B) Proliferation of miR-10b-5p transfected cells. Cell proliferation was measured at 24, 48 and 72 h, and the luminescence was compared using Welch's t-test. (C) Representative images and bar graphs of the clonogenic assay. Transfected cells were seeded in 6-well plates (300 cells/well) and incubated for 6 days, and the number of colonies was compared using Welch's t-test. (D) Cell-cycle distribution of miR-10b-5p-transfected cells. Cell-cycle distribution was calculated by FlowJo, and the cell percentage was compared using Welch's t-test. Error bars represent the standard errors of the mean. *P<0.05, **P<0.01 and ***P<0.001. miR, microRNA; NC, negative control.

in ULMS tissues compared with that in paired normal tissues (P<0.01; Fig. 1D).

Tumor-suppressive roles of miR-10b-5p in LMS cells. A gain-of-function analysis was performed to elucidate the potential roles of the downregulated miRNAs in LMS. The expression levels of miR-10b-5p were significantly increased post-transfection with the miR-10b-5p mimic (Fig. 2A). The overexpression of miR-10b-5p significantly decreased the proliferation of SK-UT-1 and SK-LMS-1 cell (P<0.01 and P<0.05; Fig. 2B). Similarly, miR-29a-3p, miR-126-3p and miR186-5p had tumor-suppressive roles; in particular, miR-126-3p significantly decreased the proliferation of SK-UT-1 and SK-LMS-1 cells (P<0.01 and P<0.001; Fig. S1A-F). The present study focused on miR-10b-5p because the baseline expression of miR-10b-5p was ~10-fold higher than that of miR-126-5p (Fig. 1C). Subsequently, the clonogenic assay revealed that miR-10b-5p overexpression significantly reduced the number of SK-UT-1 and SK-LMS-1 cell colonies (P<0.001 and P<0.001; Fig. 2C). However, soft agar colony formation assay showed that miR-10b-5p did not suppress the number of colonies (Fig. S2). In addition, the overexpression of miR-10b-5p significantly increased the population of SK-UT-1 and SK-LMS-1 cells in G_1 phase (P<0.05 and P<0.01), and decreased the population of SK-UT-1 and SK-LMS-1 cells in G_2/M phase (SK-UT-1 and SK-LMS-1; P<0.05 and P<0.01)

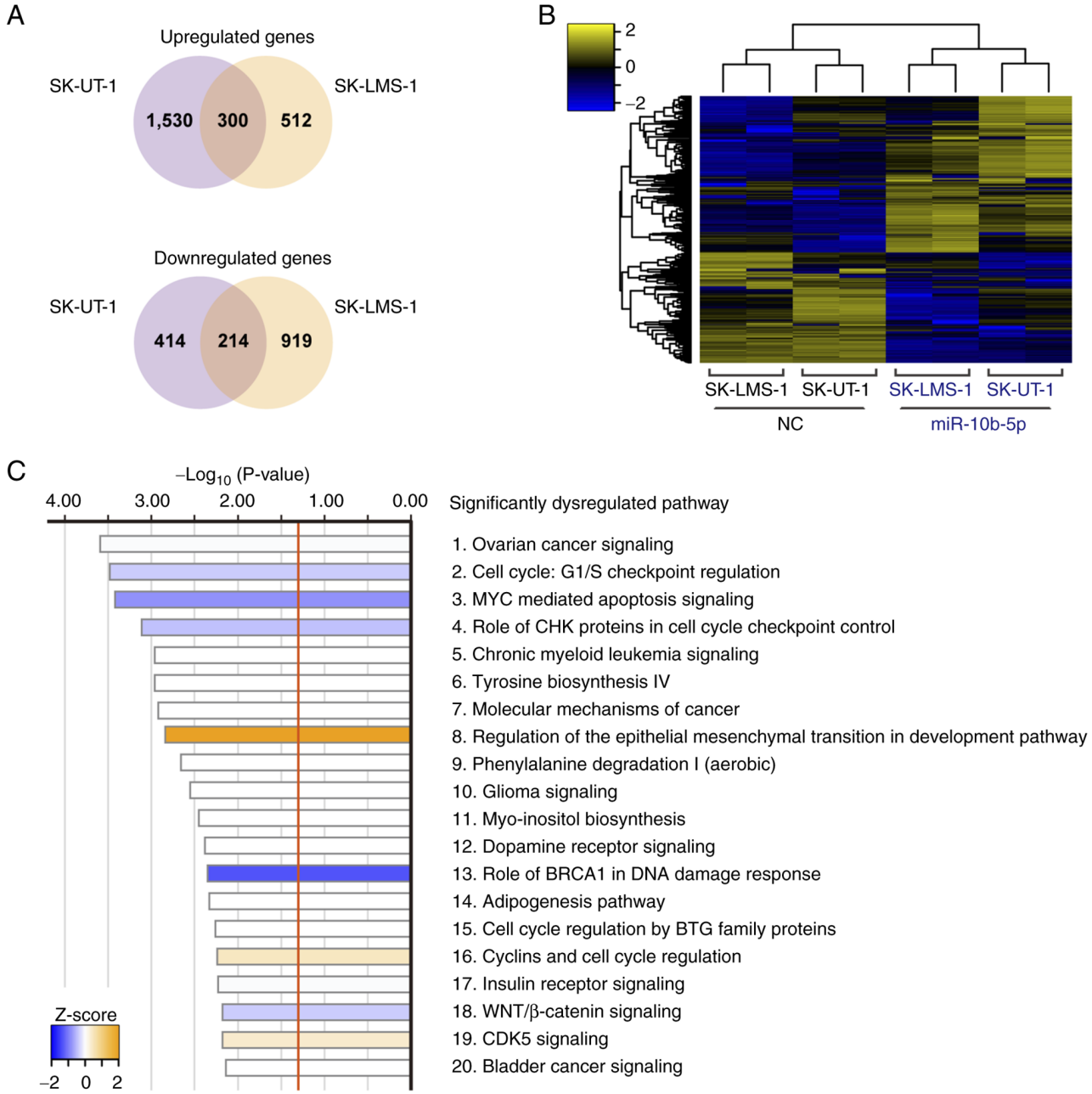

Figure 3. Transcriptome analysis of cells overexpressing miR-10b-5p. (A) Venn diagram showing dysregulated genes in common between miR-10b-5p-transfected SK-UT-1 and SK-LMS-1 cells. (B) Hierarchical clustering and heatmap showing 514 differentially expressed genes due to miR-10b-5p transfection. (C) Top 20 significantly dysregulated pathways based on Ingenuity Pathway Analysis for the 514 differentially expressed genes. miR, microRNA.

(Fig. 2D). Therefore, these results may suggest that miR-10b-5p suppressed the proliferation of LMS cells.

Potential functions of miR-10b-5p in LMS cells. Transcriptome analysis was performed to investigate the molecular background of miR-10b-5p-associated tumor suppression. miR-10b-5p-transfected SK-UT-1 cells had 1,830 upregulated and 628 downregulated genes compared with NC-transfected SK-UT-1 cells. Similarly, 812 upregulated and 1,133 downregulated genes were observed in miR-10b-5p-transfected SK-LMS-1 cells. Of these, 300 upregulated and 214 downregulated genes were identified in both cell lines (Fig. 3A). The heatmap in Fig. 3B shows the levels of 514 common DEGs in these cells. Subsequently, IPA analysis was performed using the 514 DEGs and 52 significantly dysregulated pathways were revealed (Fig. 3C; Table SII). For example, 'Cell Cycle: G1/S Checkpoint Regulation' ($P=3.31x10^{-4}$; z-score=−0.378) and 'MYC Mediated Apoptosis Signaling' ($P=3.80x10^{-4}$; z-score=−0.816) were significantly inhibited, whereas 'Regulation Of The Epithelial-Mesenchymal Transition In Development Pathway' ($P=1.45x10^{-3}$; z-score, 2.000) was significantly activated (Fig. 3C).

Discussion

ULMS is a rare tumor, the molecular biological features of which are not well understood. Consistent with the results of the present study, the expression of miR-10b-5p has been

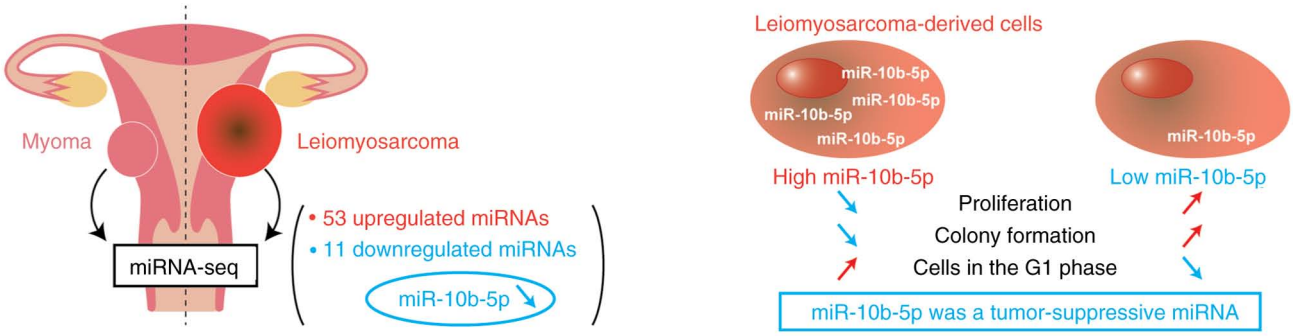

Figure 4. Schematic diagram. Comprehensive miRNA sequencing revealed that 53 and 11 miRNAs were significantly upregulated or downregulated, respectively, in uterine LMS compared with myoma. In LMS-derived cells, miR-10b-5p overexpression suppressed cell proliferation and colony formation, and increased the proportion of cells in G1 phase. These results demonstrated that miR-10b-5p had tumor-suppressive roles in LMS development. miR/miRNA, microRNA; LMS, leiomyosarcoma.

reported to be lower in several uterine sarcomas compared with that in benign uterine tissues (28). Moreover, a previous report demonstrated that miR-10b-5p was one of the downregulated miRNAs in SK-UT-1 cells compared with in myoma and myometrial cells (THESCs CRL-4003 and PCS-460-011) (29). However, to the best of our knowledge, no reports have assessed the detailed function of miR-10b-5p in ULMS cells. It is essential to investigate the functions of miRNAs in LMS-derived cells because miRNAs can have oncogenic or tumor-suppressive roles depending on the cell type. Therefore, the present study provides a novel insight into the molecular mechanism of ULMS pathogenesis.

Previously, several reports have shown the functions of miR-10b-5p in other malignancies. According to The Cancer Genome Atlas data, decreased miR-10b-5p expression is observed in various malignancies compared with in normal tissues (30). Moreover, miR-10b-5p can suppress cell proliferation and migration, and increase the rate of apoptosis by regulating *CREB1* expression in renal cancer (31). Furthermore, the overexpression of miR-10b-5p can act as a tumor suppressor in gastric cancer by targeting *TIAM1* (32,33). However, other studies have shown that miR-10b-5p can act as an oncogene by activating TGFβ signaling in gastric and breast cancer (34,35). Furthermore, miR-10b-5p has been reported to promote migration and colony formation by targeting *CDH1* in breast cancer, and the oncogenic miR-10b-5p has been revealed to target p21 and p53 in colorectal cancer (36,37). Moreover, miR-10b-5p contributes to glioma progression by targeting *HOXB3* and *WWC3* (38,39). Furthermore, miR-10b-5p, which is delivered by hypoxic glioma-derived extracellular vesicles, can accelerate macrophage M2 polarization, resulting in the progression of glioma (40). These results suggested that miR-10b-5p can have both oncogenic and tumor-suppressive roles, depending on the organ and cell type. Therefore, it is essential to investigate the functions of miR-10b-5p in ULMS. The present study demonstrated that miR-10b-5p decreased the proliferation and colony formation ability of LMS-derived cells. Moreover, cell cycle analysis revealed that overexpression of miR-10b-5p increased the number of cells in G_1 phase. The result of cell cycle analysis may be due to the prolonged doubling time of the cells, although it is difficult to determine the cell cycle speed from the present results.

miRNAs stably exist in body fluids, such as peripheral blood and urine; therefore, they are potentially non-invasive biomarkers (41). Previous reports have indicated that serum miR-10b-5p is elevated in patients with lung adenocarcinoma or hepatocellular carcinoma compared with in normal controls (42-44). In our previous microarray-based study, the serum miRNA profiles of ULMS were evaluated, and it was revealed that an index calculated using miR-191-5p and miR-1246 could be an accurate diagnostic biomarker (45). However, serum miR-10b-5p did not differ significantly between ULMS and myoma samples (45). Therefore, the expression levels of serum miR-10-5p may not be correlated with those of cellular miR-10b-5p in ULMS and myoma.

The present study has several limitations. First, the sample size was small, and the individual differences may have skewed the results of miRNA sequencing. Second, it is still controversial as to whether myoma is a suitable control for LMS. In previous reports, the miRNA signature of ULMS was compared with that of carcinosarcoma or endometrial stromal sarcoma (27,46). Moreover, miRNA profiles can differ depending on platforms, such as microarray and next-generation sequencing (47). Therefore, further studies are needed to conclude the ULMS-associated miRNA profile. Third, the direct target genes of miR-10b-5p were not assessed. It was hypothesized that miR-10b-5p may exert tumor-suppressive effects as a result of the cooperation of the various target genes; however, miR-10b-5p did not have an effect in soft agar colony formation assay. It was suggested that transient overexpression may be inappropriate for a long-term culture protocol. Fourth, the functions of other miRNAs, such as miR-29a-3p, miR-126-3p and miR-186-5p, were not fully evaluated. In addition, the *in vivo* functions of miRNAs were not assessed using animal models. Therefore, additional experiments are required to elucidate the molecular background of ULMS and to develop novel therapeutic strategies targeting miRNA-related pathways.

In conclusion, the present study identified the unique miRNA profiles of ULMS through miRNA sequencing, and the expression of miR-10b-5p was revealed to be significantly downregulated in ULMS compared with in myoma (Fig. 4). A subsequent *in vitro* analysis revealed that the overexpression of miR-10b-5p suppressed LMS cell proliferation and

colony formation, and increased the number of cells in G_1 phase. These findings suggested that miR-10b-5p may act as a tumor suppressor, and miR-10b-5p and its target genes could be novel therapeutic targets. Further elucidation of the molecular background of ULMS may improve patient prognoses.

Acknowledgements

Not applicable.

Funding

This study was supported by JSPS KAKENHI (grant nos. 21H02721, 21H03075 and 21K16789) and the Fusion Oriented Research for Disruptive Science and Technology (FOREST) from Japan Science and Technology Agency (JST). Moreover, this study was supported by the YOKOYAMA Foundation for Clinical Pharmacology (grant no. YRY-2115), the Princess Takamatsu Cancer Research Fund (grant no. 20-25237), the Mochida Memorial Foundation for Medical and Pharmaceutical Research (grant no. 202102016), Daiichi Sankyo Foundation of Life Science (grant no. 2021HrCK), the Uehara Memorial Foundation (grant no. 202110201), the Japan Research Foundation for Clinical Pharmacology (grant no. 2021A18), and the Foundation for Promotion of Cancer Research in Japan.

Availability of data and materials

The datasets generated during and/or analyzed during the current study are available from the corresponding author on reasonable request. Moreover, the raw sequencing data generated and/or analyzed during the current study are available in the Gene Expression Omnibus repository [https://www.ncbi.nlm.nih.gov/geo/query/acc.cgi?acc=GSE200777 and https://www.ncbi.nlm.nih.gov/geo/query/acc.cgi?acc=GSE201542].

Authors' contributions

KY, AY, TK, HK and YY conceived the present study. HY and TK made substantial contributions to the acquisition of data. KY, MK, MS, TY and JN performed and analyzed experiments. KY, AY and YY confirm the authenticity of all the raw data. AY, HK and YY supervised the project and were involved in the interpretation of data. KY, AY and YY acquired funding. KY wrote the original manuscript, and AY, HK and YY revised the manuscript critically for important intellectual content. All authors read and approved the final manuscript.

Ethics approval and consent to participate

The study protocol was approved by the ethics committee at National Cancer Center (approval no. 2020-160). Written informed consent was obtained from all patients.

Patient consent for publication

Not applicable.

Competing interests

The authors declare that they have no competing interests.

References

1. Skorstad M, Kent A and Lieng M: Uterine leiomyosarcoma-incidence, treatment, and the impact of morcellation. A nationwide cohort study. Acta Obstet Gynecol Scand 95: 984-990, 2016.
2. George S, Serrano C, Hensley ML and Ray-Coquard I: Soft tissue and uterine leiomyosarcoma. J Clin Oncol 36: 144-150, 2018.
3. Roberts ME, Aynardi JT and Chu CS: Uterine leiomyosarcoma: A review of the literature and update on management options. Gynecol Oncol 151: 562-572, 2018.
4. Seagle BL, Sobecki-Rausch J, Strohl AE, Shilpi A, Grace A and Shahabi S: Prognosis and treatment of uterine leiomyosarcoma: A national cancer database study. Gynecol Oncol 145: 61-70, 2017.
5. Hensley ML, Patel SR, von Mehren M, Ganjoo K, Jones RL, Staddon A, Rushing D, Milhem M, Monk B, Wang G, *et al*: Efficacy and safety of trabectedin or dacarbazine in patients with advanced uterine leiomyosarcoma after failure of anthracycline-based chemotherapy: Subgroup analysis of a phase 3, randomized clinical trial. Gynecol Oncol 146: 531-537, 2017.
6. Blay JY, Schöffski P, Bauer S, Krarup-Hansen A, Benson C, D'Adamo DR, Jia Y and Maki RG: Eribulin versus dacarbazine in patients with leiomyosarcoma: Subgroup analysis from a phase 3, open-label, randomised study. Br J Cancer 120: 1026-1032, 2019.
7. Benson C, Ray-Coquard I, Sleijfer S, Litière S, Blay JY, Le Cesne A, Papai Z, Judson I, Schöffski P, Chawla S, *et al*: Outcome of uterine sarcoma patients treated with pazopanib: A retrospective analysis based on two European organisation for research and treatment of cancer (EORTC) soft tissue and bone sarcoma group (STBSG) clinical trials 62043 and 62072. Gynecol Oncol 142: 89-94, 2016.
8. Cuppens T, Moisse M, Depreeuw J, Annibali D, Colas E, Gil-Moreno A, Huvila J, Carpén O, Zikán M, Matias-Guiu X, *et al*: Integrated genome analysis of uterine leiomyosarcoma to identify novel driver genes and targetable pathways. Int J Cancer 142: 1230-1243, 2018.
9. Hensley ML, Chavan SS, Solit DB, Murali R, Soslow R, Chiang S, Jungbluth AA, Bandlamudi C, Srinivasan P, Tap WD, *et al*: Genomic landscape of uterine sarcomas defined through prospective clinical sequencing. Clin Cancer Res 26: 3881-3888, 2020.
10. Astolfi A, Nannini M, Indio V, Schipani A, Rizzo A, Perrone AM, De Iaco P, Pirini MG, De Leo A, Urbini M, *et al*: Genomic database analysis of uterine leiomyosarcoma mutational profile. Cancers (Basel) 12: 2126, 2020.
11. Choi J, Manzano A, Dong W, Bellone S, Bonazzoli E, Zammataro L, Yao X, Deshpande A, Zaidi S, Guglielmi A, *et al*: Integrated mutational landscape analysis of uterine leiomyosarcomas. Proc Natl Acad Sci USA 118: e2025182118, 2021.
12. Shan W, Akinfenwa PY, Savannah KB, Kolomeyevskaya N, Laucirica R, Thomas DG, Odunsi K, Creighton CJ, Lev DC and Anderson ML: A small-molecule inhibitor targeting the mitotic spindle checkpoint impairs the growth of uterine leiomyosarcoma. Clin Cancer Res 18: 3352-3365, 2012.
13. Yoshida K, Yokoi A, Yamamoto T, Hayashi Y, Nakayama J, Yokoi T, Yoshida H, Kato T, Kajiyama H and Yamamoto Y: Aberrant activation of cell cycle-related kinases and the potential therapeutic impact of PLK1 or CHEK1 inhibition in uterine leiomyosarcoma. Clin Cancer Res 28: 2147-2159, 2022.
14. Ambros V: The functions of animal microRNAs. Nature 431: 350-355, 2004.
15. Kozomara A, Birgaoanu M, Griffiths-Jones S: miRBase: From microRNA sequences to function. Nucleic Acids Res 47 (D1): D155-D162, 2019.
16. Kim VN, Han J and Siomi MC: Biogenesis of small RNAs in animals. Nat Rev Mol Cell Biol 10: 126-139, 2009.
17. Esquela-Kerscher A and Slack FJ: Oncomirs-microRNAs with a role in cancer. Nat Rev Cancer 6: 259-269, 2006.
18. Garzon R, Calin GA and Croce CM: MicroRNAs in cancer. Annu Rev Med 60: 167-179, 2009.
19. Yoshida K, Yamamoto Y and Ochiya T: miRNA signaling networks in cancer stem cells. Regen Ther 17: 1-7, 2021.
20. Shi G, Perle MA, Mittal K, Chen H, Zou X, Narita M, Hernando E, Lee P and Wei JJ: Let-7 repression leads to HMGA2 overexpression in uterine leiomyosarcoma. J Cell Mol Med 13: 3898-3905, 2009.

21. Pazzaglia L, Novello C, Conti A, Pollino S, Picci P and Benassi MS: miR-152 down-regulation is associated with MET up-regulation in leiomyosarcoma and undifferentiated pleomorphic sarcoma. Cell Oncol (Dordr) 40: 77-88, 2017.
22. Love MI, Huber W and Anders S: Moderated estimation of fold change and dispersion for RNA-seq data with DESeq2. Genome Biol 15: 550, 2014.
23. Livak KJ and Schmittgen TD: Analysis of relative gene expression data using real-time quantitative PCR and the 2(-Delta Delta C(T)) method. Methods 25: 402-408, 2001.
24. Bray NL, Pimentel H, Melsted P and Pachter L: Near-optimal probabilistic RNA-seq quantification. Nat Biotechnol 34: 525-527, 2016.
25. Soneson C, Love MI and Robinson MD: Differential analyses for RNA-seq: Transcript-level estimates improve gene-level inferences. F1000Res 4: 1521, 2015.
26. Hemming ML, Fan C, Raut CP, Demetri GD, Armstrong SA, Sicinska E and George S: Oncogenic gene-expression programs in leiomyosarcoma and characterization of conventional, inflammatory, and uterogenic subtypes. Mol Cancer Res 18: 1302-1314, 2020.
27. Leitao MM Jr, Hensley ML, Barakat RR, Aghajanian C, Gardner GJ, Jewell EL, O'Cearbhaill R and Soslow RA: Immunohistochemical expression of estrogen and progesterone receptors and outcomes in patients with newly diagnosed uterine leiomyosarcoma. Gynecol Oncol 124: 558-562, 2012.
28. Gonzalez Dos Anjos L, de Almeida BC, Gomes de Almeida T, Mourão Lavorato Rocha A, De Nardo Maffazioli G, Soares FA, Werneck da Cunha I, Baracat EC and Carvalho KC: Could miRNA signatures be useful for predicting uterine sarcoma and carcinosarcoma prognosis and treatment? Cancers (Basel) 10: 315, 2018.
29. de Almeida BC, Garcia N, Maffazioli G, dos Anjos LG, Baracat EC and Carvalho KC: Oncomirs expression profiling in uterine leiomyosarcoma cells. Int J Mol Sci 19: 52, 2017.
30. Wang J, Yan Y, Zhang Z and Li Y: Role of miR-10b-5p in the prognosis of breast cancer. PeerJ 7: e7728, 2019.
31. Li Y, Chen D, Li Y, Jin L, Liu J, Su Z, Qi Z, Shi M, Jiang Z, Ni L, *et al*: Oncogenic cAMP responsive element binding protein 1 is overexpressed upon loss of tumor suppressive miR-10b-5p and miR-363-3p in renal cancer. Oncol Rep 35: 1967-1978, 2016.
32. Hu G, Shi Y, Zhao X, Gao D, Qu L, Chen L, Zhao K, Du J and Xu W: CBFβ/RUNX3-miR10b-TIAM1 molecular axis inhibits proliferation, migration, and invasion of gastric cancer cells. Int J Clin Exp Pathol 12: 3185-3196, 2019.
33. Liu F, An X, Zhao X, Zhang N, Chen B, Li Z and Xu W: MiR-10b-5p inhibits tumorigenesis in gastric cancer xenograft mice model through down-regulating Tiam1. Exp Cell Res 407: 112810, 2021.
34. Yan T, Wang X, Wei G, Li H, Hao L, Liu Y, Yu X, Zhu W, Liu P, Zhu Y and Zhou X: Exosomal miR-10b-5p mediates cell communication of gastric cancer cells and fibroblasts and facilitates cell proliferation. J Cancer 12: 2140-2150, 2021.
35. Lo PK, Zhang Y, Yao Y, Wolfson B, Yu J, Han SY, Duru N and Zhou Q: Tumor-associated myoepithelial cells promote the invasive progression of ductal carcinoma in situ through activation of TGFβ signaling. J Biol Chem 292: 11466-11484, 2017.
36. Wang B, Zhang Y, Zhang H, Lin F, Tan Q, Qin Q, Bao W, Liu Y, Xie J and Zeng Q: Long intergenic non-protein coding RNA 324 prevents breast cancer progression by modulating miR-10b-5p. Aging (Albany NY) 12: 6680-6699, 2020.
37. Lu C, Jiang W, Hui B, Rong D, Fu K, Dong C, Tang W and Cao H: The circ_0021977/miR-10b-5p/P21 and P53 regulatory axis suppresses proliferation, migration, and invasion in colorectal cancer. J Cell Physiol 235: 2273-2285, 2020.
38. Li W, Li C, Xiong Q, Tian X and Ru Q: MicroRNA-10b-5p downregulation inhibits the invasion of glioma cells via modulating homeobox B3 expression. Exp Ther Med 17: 4577-4585, 2019.
39. Yang Y, Liu X, Zheng J, Xue Y, Liu L, Ma J, Wang P, Yang C, Wang D, Shao L, *et al*: Interaction of BACH2 with FUS promotes malignant progression of glioma cells via the TSLNC8-miR-10b-5p-WWC3 pathway. Mol Oncol 14: 2936-2959, 2020.
40. Li B, Yang C, Zhu Z, Chen H and Qi B: Hypoxic glioma-derived extracellular vesicles harboring MicroRNA-10b-5p enhance M2 polarization of macrophages to promote the development of glioma. CNS Neurosci Ther 28: 1733-1747, 2022.
41. Yoshida K, Yokoi A, Kato T, Ochiya T and Yamamoto Y: The clinical impact of intra- and extracellular miRNAs in ovarian cancer. Cancer Sci 111: 3435-3444, 2020.
42. Shan X, Zhang L, Zhu DX, Zhou X, Zhang H, Liu QX, Tang JW, Wen W, Wang TS, Zhu W and Liu P: Serum microRNA expression profiling revealing potential diagnostic biomarkers for lung adenocarcinoma. Chin Med J (Engl) 133: 2532-2542, 2020.
43. Cho HJ, Eun JW, Baek GO, Seo CW, Ahn HR, Kim SS, Cho SW and Cheong JY: Serum exosomal MicroRNA, miR-10b-5p, as a potential diagnostic biomarker for early-stage hepatocellular carcinoma. J Clin Med 9: 281, 2020.
44. Ghosh S, Bhowmik S, Majumdar S, Goswami A, Chakraborty J, Gupta S, Aggarwal S, Ray S, Chatterjee R, Bhattacharyya S, *et al*: The exosome encapsulated microRNAs as circulating diagnostic marker for hepatocellular carcinoma with low alpha-fetoprotein. Int J Cancer 147: 2934-2947, 2020.
45. Yokoi A, Matsuzaki J, Yamamoto Y, Tate K, Yoneoka Y, Shimizu H, Uehara T, Ishikawa M, Takizawa S, Aoki Y, *et al*: Serum microRNA profile enables preoperative diagnosis of uterine leiomyosarcoma. Cancer Sci 110: 3718-3726, 2019.
46. Ravid Y, Formanski M, Smith Y, Reich R and Davidson B: Uterine leiomyosarcoma and endometrial stromal sarcoma have unique miRNA signatures. Gynecol Oncol 140: 512-517, 2016.
47. Git A, Dvinge H, Salmon-Divon M, Osborne M, Kutter C, Hadfield J, Bertone P and Caldas C: Systematic comparison of microarray profiling, real-time PCR, and next-generation sequencing technologies for measuring differential microRNA expression. RNA 16: 991-1006, 2010.